



RESEARCH LETTER

10.1002/2016GL068207

Key Points:

- Direct observation of a photochemical source of HNCO from diesel exhaust
- Secondary production of HNCO from diesel exhaust is more important after a day of atmospheric aging than the primary emission source
- Primary emissions and secondary formation of HNCO are higher for idle engine loads than active engine loads

Supporting Information:

- Supporting Information S1

Correspondence to:

D. K. Farmer,
delphine.farmer@rams.colostate.edu

Citation:

Link, M. F., B. Friedman, R. Fulgham, P. Brophy, A. Galang, S. H. Jathar, P. Veres, J. M. Roberts, and D. K. Farmer (2016), Photochemical processing of diesel fuel emissions as a large secondary source of isocyanic acid (HNCO), *Geophys. Res. Lett.*, *43*, 4033–4041, doi:10.1002/2016GL068207.

Received 9 FEB 2016

Accepted 20 MAR 2016

Published online 26 APR 2016

Photochemical processing of diesel fuel emissions as a large secondary source of isocyanic acid (HNCO)

M. F. Link¹, B. Friedman¹, R. Fulgham¹, P. Brophy¹, A. Galang², S. H. Jathar², P. Veres^{3,4}, J. M. Roberts⁴, and D. K. Farmer¹

¹Department of Chemistry, Colorado State University, Fort Collins, Colorado, USA, ²Department of Mechanical Engineering, Colorado State University, Fort Collins, Colorado, USA, ³Cooperative Institute for Research in Environmental Sciences, Boulder, Colorado, USA, ⁴Chemical Sciences Division, NOAA Earth System Research Laboratory, Boulder, Colorado, USA

Abstract Isocyanic acid (HNCO) is a well-known air pollutant that affects human health. Biomass burning, smoking, and combustion engines are known HNCO sources, but recent studies suggest that secondary production in the atmosphere may also occur. We directly observed photochemical production of HNCO from the oxidative aging of diesel exhaust during the Diesel Exhaust Fuel and Control experiments at Colorado State University using acetate ionization time-of-flight mass spectrometry. Emission ratios of HNCO were enhanced, after 1.5 days of simulated atmospheric aging, from 50 to 230 mg HNCO/kg fuel at idle engine operating conditions. Engines operated at higher loads resulted in less primary and secondary HNCO formation, with emission ratios increasing from 20 to 40 mg HNCO/kg fuel under 50% load engine operating conditions. These results suggest that photochemical sources of HNCO could be more significant than primary sources in urban areas.

1. Introduction

Atmospherically relevant levels of isocyanic acid (HNCO) are expected to be toxic at biological pH [Roberts *et al.*, 2011]. Toxic effects of HNCO are associated with cataracts, atherosclerosis, cardiovascular disease, renal failure, and rheumatoid arthritis [Jaisson *et al.*, 2011]. Roberts *et al.* [2011] estimated exposure to only 1 ppbv HNCO could produce aqueous isocyanate in the body, which can trigger harmful protein-modifying processes [Wang *et al.*, 2007; Mydel *et al.*, 2010; Verbrugge *et al.*, 2015]. Previous studies have recognized the occupational hazard of exposure to isocyanates, including HNCO, and have measured mixing ratios of HNCO near 1 ppbv in different workplace environments [Karlsson *et al.*, 2001; Sennbro *et al.*, 2004; Westberg *et al.*, 2005] underscoring the need to characterize its sources. Observations of HNCO have been performed from direct sources such as light-duty gasoline vehicle emissions [Brady *et al.*, 2014], light-duty diesel vehicle emissions [Wentzell *et al.*, 2013], biomass burning [Roberts *et al.*, 2011], and from secondary sources such as the photochemical oxidation of 2-aminoethanol [Borduas *et al.*, 2013] and the aqueous dissociation of urea [Verbrugge *et al.*, 2015]. Studies in the ambient environment [Wentzell *et al.*, 2013; Roberts *et al.*, 2014; Woodward-Massey *et al.*, 2014; Zhao *et al.*, 2014] have correlated HNCO with photochemically produced species such as ozone, formic acid, and nitric acid, which is consistent with a photochemical source of HNCO. However, direct measurements of the photochemical production of HNCO have only been made in laboratory studies from isolated precursors such as 2-aminoethanol [Borduas *et al.*, 2013]. While modeled HNCO production from 2-aminoethanol oxidation only accounted for 14% of ambient measured HNCO in one study [Karl *et al.*, 2015], ambient mixing ratios of formamide, can account for almost all observed HNCO in some rural environments [Roberts *et al.*, 2014; Sarkar *et al.*, 2015].

Emissions from nonroad diesel engines have received less attention than emissions from on-road vehicles. Nonroad diesel vehicles contributed 18% and 15% to PM₁₀ and nitrogen oxide (NO_x) emissions, respectively, in the United States in 2011 [Environmental Protection Agency, 2011]. Previous studies have demonstrated that diesel exhaust is also a primary source of HNCO [Heeb *et al.*, 2011; Wentzell *et al.*, 2013]. The most recent Environmental Protection Agency (EPA) Tier 4 standards of emissions reduction regulations have focused on the reduction of NO_x by requiring all nonroad diesel vehicles produced after 2015 to be equipped with selective catalytic reduction systems (SCR) in addition to particle-reducing filters and hydrocarbon oxidation catalysts required by previous emission control mandates. The addition of SCR systems to diesel vehicles are known to produce HNCO as an intermediate in the NO_x reduction process which has resulted in higher emission factors of HNCO observed than without the addition of the SCR system [Heeb *et al.*, 2012].

Wentzell *et al.* [2013] measured HNCO emissions from light-duty diesel engine exhaust and concluded that diesel engine emissions in the greater Toronto area are smaller HNCO sources than biomass burning throughout Canada. They speculated, however, that HNCO emissions from heavy-duty diesel vehicles and nonroad use of diesel may be much larger as these sources are dominant contributors to total mobile source pollution [Wentzell *et al.*, 2013].

Here we investigate secondary production of HNCO by simulating photochemical oxidation (or aging) of diesel and biodiesel exhaust from a nonroad diesel engine, and the extent to which this chemistry enhances the HNCO source from diesel exhaust. Despite regulatory controls in the U.S., urban air pollution remains a public health concern, particularly for highly sensitive groups [Correia *et al.*, 2013]. Primary diesel particle emissions, and their resulting secondary chemistry, have long been recognized as source of urban air pollution [Robinson *et al.*, 2007], but here we investigate the role of photochemically enhanced HNCO diesel engine emissions.

2. Materials and Methods

2.1. Experimental Set up

The Diesel Exhaust Fuel and Control (DEFCON) experiment took place at the Colorado State University Engines and Energy Conversion Laboratory during 3–11 June 2015. A four-cylinder, turbocharged, inter-cooled, heavy-duty diesel engine (John Deere 4045H), representative of those found in skid-steer loaders, tractors, etc., was run on an engine dynamometer under idle and 50% load operating conditions using both diesel (sulfur content 6–10 ppm) and biodiesel fuels to produce exhaust. No emissions control systems—including diesel oxidation catalyst, diesel particulate filter, nor SCR unit—were included in the experiments described herein. Raw exhaust was transferred through 4 m of heated Silcosteel copyright stainless steel line to a primary dilution system [Quillen *et al.*, 2008]. The exhaust was mixed with high-efficiency particulate arrestance (HEPA) filtered and activated charcoal- filtered room air (Figure S1.1 in the supporting information) to achieve dilution ratios of 45–110 (air:exhaust). The diluted exhaust was transferred to a 300 L stainless steel tank and had a residence time in the equilibration tank of 10 min before undergoing continuous sampling. Diluted engine exhaust is subsampled to the potential aerosol mass (PAM) reactor where oxidation occurs, and this sample air is directed to both particle and gas phase instruments on different sampling lines (Figure S1.1). Mixing ratios of CO₂, CO, total hydrocarbons (THC), NO, and NO₂ were measured by a five-gas analyzer [Quillen *et al.*, 2008] from the primary engine exhaust upstream of the dilution chamber (Table S1.2).

The diluted sample exhaust was introduced into a potential aerosol mass (PAM) reactor [Kang *et al.*, 2007; Lambe *et al.*, 2011] to simulate atmospheric oxidation at a flow rate of 7 standard liters per minute (sLpm) (residence time ~100 s). The PAM reactor is a 13.1 L conductive aluminum chamber equipped with high-pressure mercury lamps (BHK Inc., model # 82-9304-03) to simulate atmospheric HO₂ and OH oxidation chemistry. UV light is emitted at 185 and 254 nm in the reactor and initiates the production of hydroxyl radicals (OH) from the photolysis of O₂ and H₂O. The concentration of OH depends on the UV intensity emitted by the lamps and can simulate atmospheric aging of hours to weeks [Kang *et al.*, 2007].

The high reactivity ($\sim 5000 \text{ s}^{-1}$) of the diesel exhaust suppressed OH by a factor of 2 at the lowest UV light intensities and 14 at the highest intensities (see supporting information for detailed calculations), comparable to the OH suppression observed during PAM experiments on biomass burning emissions [Ortega *et al.*, 2013]. The factor contributing most to variability in the estimated OH reactivity of the diesel exhaust in the PAM chamber was the dilution of the exhaust sample in the dilution chamber. The OH exposure in the PAM chamber is typically described in terms of equivalent days of OH exposure [Lambe *et al.*, 2011; Li *et al.*, 2015; Peng *et al.*, 2015], which is calculated by dividing the OH exposure (molecules cm⁻³ s) by an average atmospheric OH concentration ($1.5 \times 10^6 \text{ molecules cm}^{-3}$ [Mao *et al.*, 2008]). The experiments described herein cover oxidative aging by OH of 0.2–1.5 ($\pm 50\%$) equivalent days of OH exposure (OH_{exp}) (Figure S2.3).

2.2. Exhaust Experiments

We measured HNCO from engine emissions during six different experiments: two replicates of diesel fuel with engine at idle, two replicates of diesel fuel with engine at 50% load, one experiment with biodiesel fuel and engine at idle, and one experiment with biodiesel fuel and engine at 50% load. Each experiment

consisted of six steps of increasing UV light voltage in the PAM chamber; each voltage step was held for 20 min. The 0 V voltage step in the PAM represents the exhaust exposed to no UV light.

2.3. Acetate-CIMS Operation and Calibration

HNCO was detected by a high-resolution time-of-flight acetate chemical ionization mass spectrometer (acetate-CIMS) (Tofwerk AG and Aerodyne Research, Inc.). The ionization chemistry [Veres *et al.*, 2008; Roberts *et al.*, 2010; Wentzell *et al.*, 2013; Brady *et al.*, 2014] and instrument [Brophy and Farmer, 2015] have been described extensively in previous literature. Sample air for gas phase analytes was pulled through 3 m of PEEK tubing from the PAM chamber to the acetate-CIMS and diluted at the entrance to the instrument by 3.6 sLpm of ultrahigh-purity N₂ to maintain first-order reactions of the analytes in the sample gas with the acetate reagent ion. The acetate-CIMS pulled sample air through a critical orifice (ID 0.067 cm) at a flow rate of 1.5 sLpm. Thus, the emissions were diluted by a factor of 1200–3500 (air:exhaust) between the engine tailpipe and the instrument. Despite this large dilution, the reagent ion signal was titrated by large signals observed at m/z 45.99 (NO₂[−]) and m/z 61.99 (NO₃[−]) throughout the experiments, likely due to HONO and HNO₃, respectively. HNCO can be ionized through either a proton transfer or clustering reaction with acetate (Ac[−]),



The ion optics in the negative ion (NI)-(proton transfer) PT-CIMS were tuned to minimize clustering in the observed spectra [Brophy and Farmer, 2015] so that HNCO is detected as NCO[−] at m/z 41.99. No interfering species at same nominal mass as HNCO were observed through peak fitting procedures either during calibration or during the DEFCON experiments.

We calibrated the NI-PT-CIMS for HNCO with a stable source of HNCO that was produced by passing a stream of zero air at 50 cm³ min^{−1} STP over the outlet of a diffusion cell containing heated cyanuric acid (250°C) [Roberts *et al.*, 2010]. HNCO concentrations were determined with a custom-built analyzer that converts HNCO to NO on a heated platinum catalyst (750°C) followed by a molybdenum catalyst (450°C) and detects NO via chemiluminescence [Veres and Roberts, 2015]. The NI-PT-CIMS had a sensitivity to HNCO of 47.5 normalized counts per second/parts per trillion by volume (pptv) and a detection limit (S/N = 3) for HNCO of 5 pptv at 1 s acquisition (supporting information for additional calibration details).

2.4. Calculation of Fuel-Based EEF_ts

Fuel-based emission factors have been recognized as a useful metric for comparing engines operating under different conditions but using similar fuels [Brady *et al.*, 2014]. Emission factors (EFs, mg HNCO/kg fuel) were first calculated by

$$\text{EF} = \frac{[\text{HNCO}]}{\left(\frac{[\text{CO}_2]}{\text{MW}_{\text{CO}_2}} + \frac{[\text{CO}]}{\text{MW}_{\text{CO}}}\right) \text{AW}_C} C_i \quad (1)$$

where concentrations are in mg cm^{−3} (HNCO) or g cm^{−3} (CO and CO₂); C_i is the carbon mass fraction of the fuel (850 and 770 gC/kg fuel for diesel and biodiesel, respectively [Gordon *et al.*, 2014]); and MW_{CO₂}, MW_{CO}, and AW_C are the molecular weights of CO₂ and CO, and the atomic weight of carbon. All concentration values used in the EF calculation were calculated from the dilution ratio in the dilution chamber to produce tailpipe exhaust emission concentrations. We define fuel-based enhanced emission factors (EEF_ts, mg HNCO/kg fuel) as the HNCO produced from a given amount of fuel via atmospheric aging of diesel exhaust. EEF_ts thus describe the extent of pollutant production from a given photochemical oxidation of engine exhaust originating from the combustion of a known amount of fuel. The EEF_t of a pollutant is a function of photochemical exposure and will vary with time the pollutant spends in the atmosphere. EEF_ts were calculated to quantify the contribution of secondary production of HNCO from primary exhaust. EEF_ts were then calculated via equation (2):

$$\text{EEF}_t = \text{EF}_{\text{voltage step}} - \text{EF}_{0\text{V step}} \quad (2)$$

where EF_{voltage step} is the EF for HNCO at a given UV light voltage step and EF_{0V step} is the EF for HNCO at the UV light voltage step representative of diesel exhaust unperturbed by oxidation. The EEF_t is defined as a difference from the EF at the 0 V step in order to separate the primary HNCO emission from the secondary HNCO formation.

Table 1. EFs and EEFs After 1.5 Days of Photochemical Aging ($EEF_{1.5 \text{ days}}$) for Both Fuel Types and Under Both Engine Operating Conditions^a

	Idle		50% Load	
	EF (mg HNCO/kg fuel)	$EEF_{1.5 \text{ days}}$ (mg HNCO/kg fuel)	EF (mg HNCO/kg fuel)	$EEF_{1.5 \text{ days}}$ (mg HNCO/kg fuel)
Diesel	54 ± 3	183 ± 13	17 ± 1	26 ± 2
Biodiesel	54 ± 1	187 ± 17	17 ± 2	10 ± 2

^aThe EF describes primary emission of HNCO from the combustion of the fuel, whereas the $EEF_{1.5 \text{ days}}$ describes how much HNCO is photochemically produced after 1.5 days of aging. The total emission of HNCO from the combustion of a given fuel source ($EF + EEF_{1.5 \text{ days}}$) contributed from both primary emission and secondary formation of HNCO are shown in Figure S4.1.

3. Results and Discussion

3.1. Primary Emission of HNCO

EFs were within experimental error of one another for diesel and biodiesel under the same engine operating conditions (Table 1).

EFs were, however, 3 times larger for idle engine conditions (54 mg HNCO/kg diesel fuel) versus 50% load conditions (17 mg HNCO/kg fuel). EFs reported in the study herein are considerably higher than those reported in previous literature. EFs for HNCO reported by *Heeb et al.* [2011] were similar between engine operating conditions at 4 mg HNCO/kg of diesel fuel for on-road light-duty engines. Similarly, *Brady et al.* [2014] measured EFs for HNCO on the order of 1–2 mg HNCO/kg of gasoline fuel for light-duty gasoline vehicles. We note that *Wentzell et al.* [2013] observed a difference in primary HNCO emission as a function of engine operating condition, but with higher EFs (4.0 mg HNCO/kg diesel fuel) during active engine operating conditions and lower EFs (0.7 mg HNCO/kg diesel fuel) for idle conditions. Our data suggest that nonroad diesel engines produce more primary HNCO than either the on-road light-duty gasoline or diesel engines described in previous studies. Further, this type of engine produces much wider ranging primary HNCO emissions than reported for other engine types. These comparisons suggest that similar engine operating conditions may produce different effects on the emissions between nonroad diesel engines, such as the one used in this study, and on-road diesel engines like those used in previous studies.

Idle operating conditions generally result in less efficient combustion than more active engine operating conditions such as the 50% load conditions in this study as evidenced by the difference in THC concentration between operating conditions (Table S1.2). Our observations suggest that incomplete combustion can also be accompanied by increased primary HNCO emissions. This suggests that more precursors for HNCO could be available in the incompletely combusted exhaust under idle conditions than 50% load conditions [*Chin et al.*, 2012]. Emissions of CO, NO_x, and THC measured from the engine in this study agree well with measurements reported from the same engine in another study [*Drenth et al.*, 2014] suggesting that the emissions from this engine are reproducible. The CO mixing ratios measured in this study are nearly twice as high as those measured by *Wentzell et al.* [2013] under similar (idle) engine operating conditions, consistent with our observations of higher primary HNCO. The lower bound of the variability of THC measured in this study under idle conditions captures the average THC mixing ratio measured by *Wentzell et al.* [2013]. In contrast, *Wentzell et al.* [2013] reports NO_x emissions that are larger by a factor of 6–7 than the NO_x measured in this study. Indeed, the HNCO/NO_x ratios measured in this study (Table S4.3) are much higher than the ratios reported in *Wentzell et al.* [2013].

Previous studies have shown that steady state engine cycles, such as those used in this study, can underestimate and misrepresent emissions of particles [*Karjalainen et al.*, 2015] as well as pollutants such as HNCO. For instance, *Brady et al.* [2014] measured the highest emissions of HNCO during acceleration from gasoline exhaust. By measuring HNCO from steady state engine conditions, we are providing a lower bound to what can be expected for real-world emissions of HNCO from nonroad diesel engines. Unlike on-road vehicles, nonroad vehicles typically operate at steady state, either idle or peak, engine loads. This suggests that the HNCO emissions presented herein are similar to what could be expected from real-world engine performance.

3.2. Secondary Source of HNCO

We observe a strong secondary source of HNCO from diesel engine exhaust as a result of 0.4 to 1.5 days of photochemical aging for both biodiesel and diesel fuel and under both idle and high load operating

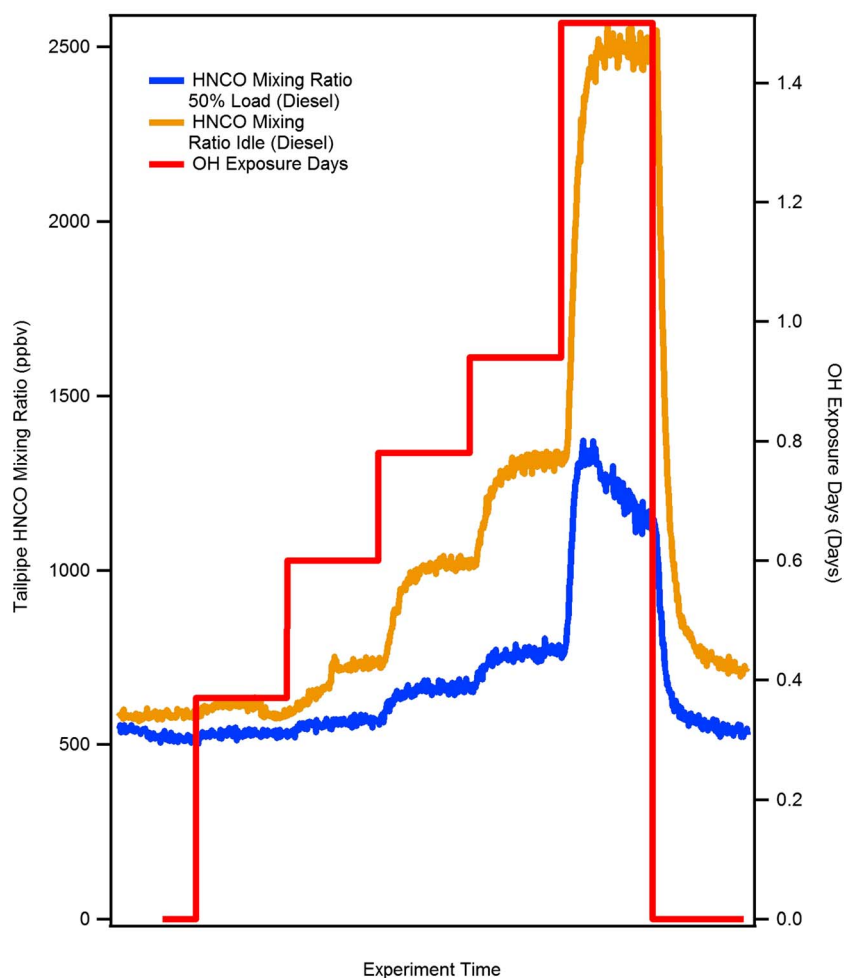


Figure 1. HNCO mixing ratio (ppbv) during a typical PAM oxidation experiment under idle (orange) and 50% load (blue) engine operating conditions with diesel fuel. Increasing UV light voltage increases the OH_{exp} (red).

conditions. Oxidation of diesel exhaust in the PAM chamber produced HNCO, enhancing observed concentrations by up to a factor of 4 (Figures 1 and S4.1). All fuel types and engine operating conditions demonstrated similar behavior with photochemical enhancement of HNCO. Figure 1 shows an example of secondary HNCO production from diesel under idle and 50% load engine operating conditions. HNCO consistently increased with photochemical exposure.

Idle conditions produced consistently higher HNCO mixing ratios than 50% load operating conditions.

EEF_{S} of secondary HNCO from photochemical oxidation of diesel and biodiesel exhaust increase as a function of OH exposure under idle and 50% load conditions (Figure 2).

EEF_{S} of HNCO were higher under idle engine operating conditions than 50% load conditions for both fuels. Under idle conditions, HNCO emissions were enhanced by a factor of 4 after 1.5 OH equivalent days. This enhancement is the equivalent of 230 mg HNCO per kg of fuel, compared to primary emissions of 54 mg HNCO/kg of fuel (Figure S4.2). In contrast, the HNCO emissions were only enhanced by a factor of 1.5–3 after 1.5 OH equivalent days under 50% load conditions, or an increase of 26 mg HNCO/kg fuel. We hypothesize that HNCO EEF_{S} are higher under idle conditions because there are more precursors for photochemical production available in incompletely combusted diesel exhaust (Figure S4.4).

3.3. Implications for Diesel Emission Reduction Technologies

Primary emissions of HNCO have been observed to be higher in the exhaust of diesel systems equipped with SCR (or de- NO_x) systems. Heeb *et al.* [2011] measured HNCO from diesel exhaust filtered through a de- NO_x

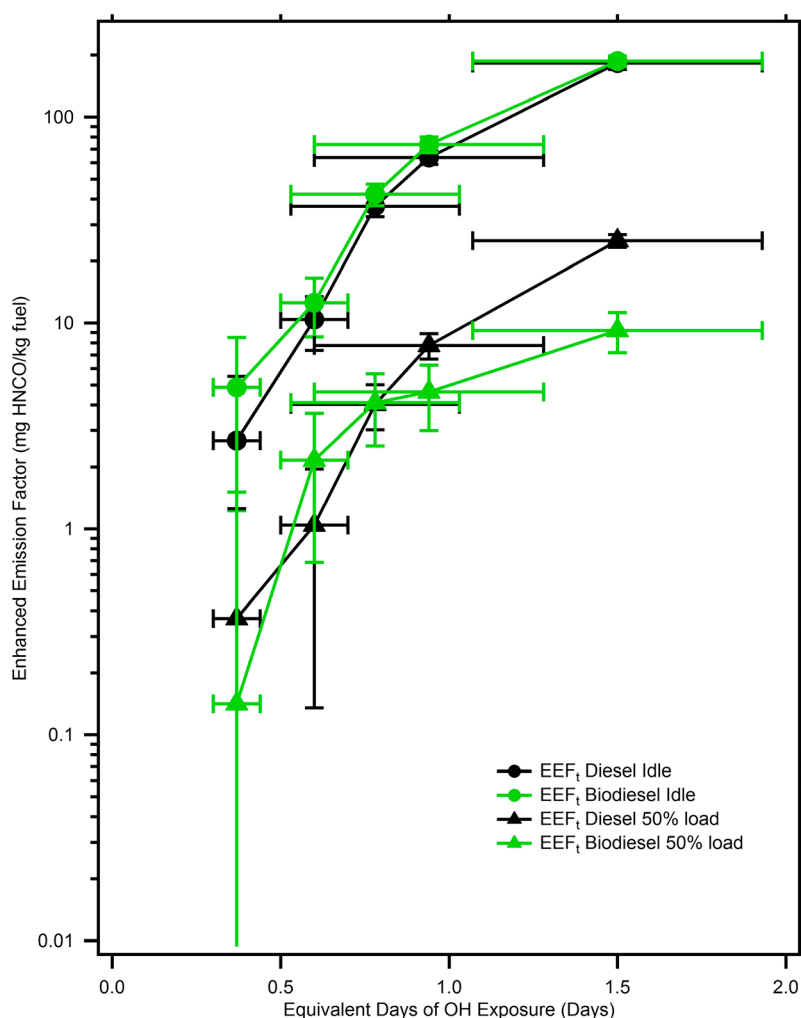


Figure 2. EEF_Ts of HNCO plotted against OH_{exp} (assuming average [OH] = 1.5×10^6 molecules cm⁻³) for biodiesel (green) and diesel (black) fuels under idle (circles) and 50% load (triangles) engine operating conditions. Vertical error bars represent the errors in measured mixing ratios of HNCO, CO₂, and CO propagated throughout the calculations of EFs and EEF_Ts. Horizontal error bars are the ± 1 standard deviation of the output from the OH_{exp} estimation model (Figure S2.3).

system and observed an increase in primary HNCO emissions by almost an order of magnitude under engine conditions similar to primary emissions observed in this study (from 3 to 79 mg HNCO/kg fuel). Kröcher *et al.* [2005] also reported tailpipe mixing ratios of HNCO much higher than those measured in this study (16–80 ppmv) with the use of a de-NO_x system. The decomposition of urea to HNCO and the subsequent hydrolysis of HNCO are temperature and catalyst dependent often resulting in emission of HNCO from the inefficient operation of the SCR system known as “HNCO slip” [Kröcher *et al.*, 2005]. Future studies should investigate the photochemical enhancement of HNCO from diesel exhaust treated with EPA Tier 4 emission abatement technologies such as diesel particle filters, oxidation catalysts, and SCRs.

Changing the composition of diesel fuel to biodiesel has been suggested to reduce emissions from older diesel vehicles that are not equipped with emissions control technologies [Varatharajan and Cheralathan, 2012]. While changing the composition of diesel fuel has been shown to be useful in reducing particle emissions [Lapuerta *et al.*, 2008], we demonstrate here that changing the composition of diesel fuel may not have a significant effect on reducing primary or secondary emissions of other pollutants such as HNCO.

3.4. Atmospheric Relevance

We evaluate the relative contributions of primary vehicle emissions and secondary sources for the California South Coast Air Basin (SoCAB) as well as California statewide wildfire sources to total HNCO emissions in

Table 2. Comparison of Mobile and Statewide Wildfire HNCO Sources Calculated From Reported CO Emissions by the CARB Projected for 2015^a

Emission Source	CO Emissions (tonnes/d)	HNCO Emissions (tonnes/d)	Secondary HNCO Emissions (tonnes/d) ^b
On-road light-duty gasoline vehicles ^c	881	0.04	0.12
On-road light-duty diesel vehicles ^d	5	0.02	0.06
Nonroad use of diesel ^e	619	2.76	8.28
Total mobile sources and nonroad sources	1505	2.82	8.46
Wildfires (statewide) ^f	4787	5.14	NA

^aPhotochemically enhanced HNCO emissions describe total emissions of HNCO from mobile sources after ~1.5 equivalent days of atmospheric aging. NA: not available.

^bEnhanced HNCO emissions are calculated by multiplying primary mobile source HNCO emissions by a photochemical enhancement factor of 3 based on our observations for 1.5 OH equivalent days of aging. While this represents a lower bound for oxidative production, as precursor molecules may have lifetimes longer than 1.5 days, we note that this estimate ignores the role of deposition, which may rapidly remove HNCO precursors from the atmosphere.

^cHNCO emissions are calculated using an average HNCO/CO ratio of 0.028 mmol HNCO mol CO⁻¹ calculated from the work of *Brady et al.* [2014] measured from light-duty gasoline vehicles.

^dHNCO emissions are calculated using HNCO/CO ratio of 2.3 mmol HNCO mol CO⁻¹ reported by *Wentzell et al.* [2013] for a light-duty diesel engine.

^eHNCO emissions are calculated using an average HNCO/CO ratio of 2.9 mmol HNCO mol CO⁻¹ measured in this study from a nonroad diesel engine.

^fHNCO emissions were calculated using an average HNCO/CO ratio of 0.7 mmol HNCO mol CO⁻¹ reported in [*Veres et al.*, 2010].

Table 2. Contributions of HNCO to this airshed from different mobile sources include on-road light-duty gasoline vehicles (using an average HNCO/CO ratio calculated from the work of *Brady et al.* [2014]) and on-road light-duty diesel vehicles [*Wentzell et al.*, 2013], as well as contributions from nonroad use of diesel (nonroad diesel engines are assumed to be representative of the engine used in this study), using an average HNCO/CO measured in this study, were evaluated from emissions reports estimates published in 2013 [*California Environmental Protection Agency Air Resources Board*, 2013]. Inclusion of on-road light-duty gasoline vehicles, nonroad use of diesel and on-road light-duty diesel accounts for 80% of total CO emissions from mobile sources reported by the California Air Resources Board (CARB) project emissions for 2015 totaling 1505 tonnes/d. The largest sources of CO excluded from this calculation are from on-road medium duty trucks and recreational boats which accounts for ~17% of total reported CO emissions. Using HNCO/CO ratios for the respective vehicle types, HNCO is calculated to be emitted in the greatest abundance by the nonroad use of diesel (Table 2).

Although light-duty gasoline vehicles contribute >55% to the total CO emissions from mobile sources in this estimate, they contribute <2% of the HNCO directly emitted from mobile sources. Total mobile sources of HNCO emissions in SoCAB are less than statewide emissions from wildfires. If the HNCO emissions from mobile sources are assumed to be enhanced by a factor of 3, as measured in this study from 1.5 OH equivalent days of atmospheric aging, then the secondary photochemical production of HNCO from mobile sources becomes several tons per day greater than primary contributions from wildfires. Previous modeling has suggested that the most important anthropogenic source of HNCO to the atmosphere is biomass burning [*Young et al.*, 2012], but here we provide evidence to suggest secondary production of HNCO, from anthropogenic sources, may be more important than primary sources in certain regions. Further, we speculate that secondary production of HNCO from biomass burning precursors is likely to be a large global source of HNCO due to the large amount of reduced nitrogen potentially released to the atmosphere during fire events.

The estimates of secondary production of HNCO presented in Table 2 may represent an upper bound for HNCO production from these sources because sinks for HNCO are not considered. The above estimate assumes that all the precursors leading to secondary HNCO production from these sources are oxidized to form HNCO as opposed to being lost through deposition or uptake to aerosol surfaces. Additionally, we assume that exhaust from all the emission sources included in this estimate experience photochemical enhancements of HNCO similar to the exhaust measured in this study. The above estimates, however, may represent a lower bound because our observations of photochemical production are limited to 1.5 days of equivalent OH exposure. Experiments that observe HNCO production within a greater range of OH_{exp} could provide insight into more realistic upper bounds of photochemical production. Other precursor compounds for photochemically produced HNCO, such as 2-aminoethanol [*Borduas et al.*, 2013] and formamide [*Barnes et al.*, 2010], have been

suggested to be important for contributing to ambient atmospheric HNCO and were not included in this estimate. Possible precursors for secondary HNCO production include formamide and acetamide, which were observed during the diesel, but not biodiesel, experiments. A rough estimate of formamide and acetamide concentrations suggests that they could account for up to ~15% of the observed HNCO in the diesel experiments (Text S4.4 for further discussion of this analysis and uncertainties). Importantly, the nitrogen-containing organic species were observed to have clear secondary photochemical sources, suggesting that HNCO may be the result of multiple generations of oxidation; the precursors for formamide and acetamide in the diesel mixture are not known at this time. Other nitrogen-containing organic compounds must contribute to HNCO photochemical production in the biodiesel experiments, and potentially to the diesel experiments as well. Further investigation into the emissions of such compounds and their chemistry is warranted. Studies focusing on the photochemical production of HNCO from biomass burning emissions as well as different vehicle sources would help clarify the precise contribution of secondary HNCO to the total atmospheric burden.

4. Conclusions

We present a direct observation of a photochemical source of HNCO from nonroad diesel engine exhaust. This photochemical source is larger than the primary emission source, consistent with previous ambient HNCO observations [Roberts *et al.*, 2014; Zhao *et al.*, 2014]. Both primary emissions and secondary production of HNCO were observed to be higher under idle engine operating conditions compared to active conditions. No difference in primary emissions or secondary production of HNCO was observed through the use of diesel or biodiesel as a fuel source. While localized emissions of HNCO, either from biomass burning or mobile sources, greatly influence mixing ratios observed in ambient air, we suggest that photochemical production of HNCO could be a dominant contributor to regional HNCO budgets, and potentially to the global burden of HNCO.

An understanding of HNCO sources is essential for predicting human health effects and for identifying controllable sources. This study demonstrates that compounds that are normally thought of as having primary sources from mobile combustion sources can be enhanced through secondary processing in the atmosphere. Inclusion of secondary pollutant sources in emissions regulation may lead to a more accurate portrayal of the potential impact of mobile sources or emissions control procedures on regional air quality.

Acknowledgments

We acknowledge an Arnold and Mabel Beckman Young Investigator Award for funding this work. Fees associated with the engine dynamometer tests (engine operation, equipment rental, fuel, and personnel) were supported through Shantanu Jathar's startup funds as new faculty hire at Colorado State University. We would like to thank Kirk Evans for technical support and undergraduate researchers Liam Lewane and Nathan Reed for test support during the campaign. The NOAA/Earth Systems Research Laboratory Chemical Sciences Division effort was supported by the NOAA Health of the Atmosphere Initiative. Any data presented and analyzed in this study can be acquired per request to the corresponding author. Detailed discussions of measurements and analysis are in the supporting information.

References

- Barnes, I., G. Solignac, A. Mellouki, and K. H. Becker (2010), Aspects of the atmospheric chemistry of amides, *ChemPhysChem*, 11(18), 3844–3857, doi:10.1002/cphc.201000374.
- Borduas, N., J. P. D. Abbatt, and J. G. Murphy (2013), Gas phase oxidation of monoethanolamine (MEA) with OH radical and ozone: Kinetics, products, and particles, *Environ. Sci. Technol.*, 47(12), 6377–6383, doi:10.1021/es401282j.
- Brady, J. M., T. A. Crisp, S. Collier, T. Kuwayama, S. D. Forestieri, V. Perraud, Q. Zhang, M. J. Kleeman, C. D. Cappa, and T. H. Bertram (2014), Real-time emission factor measurements of isocyanic acid from light duty gasoline vehicles, *Environ. Sci. Technol.*, 48(19), 11,405–11,412, doi:10.1021/es504354p.
- Brophy, P., and D. K. Farmer (2015), A switchable reagent ion high resolution time-of-flight chemical ionization mass spectrometer for real-time measurement of gas phase oxidized species: Characterization from the 2013 southern oxidant and aerosol study, *Atmos. Meas. Tech.*, 8(7), 2945–2959, doi:10.5194/amt-8-2945-2015.
- California Environmental Protection Agency Air Resources Board (2013), Almanac emission projection data: 2015 estimated annual average emissions.
- Chin, J.-Y., S. A. Batterman, W. F. Northrop, S. V. Bohac, and D. N. Assanis (2012), Gaseous and particulate emissions from diesel engines at idle and under load: Comparison of biodiesel blend and ultralow sulfur diesel fuels, *Energy Fuels*, 26(11), 6737–6748, doi:10.1021/ef300421h.
- Correia, A. W., C. A. Pope, D. W. Dockery, Y. Wang, M. Ezzati, and F. Dominici (2013), The effect of air pollution control on life expectancy in the United States: An analysis of 545 US counties for the period 2000 to 2007, *Epidemiology*, 24(1), 23–31, doi:10.1097/EDE.0b013e3182770237.
- Drenth, A. C., D. B. Olsen, P. E. Cabot, and J. J. Johnson (2014), Compression ignition engine performance and emission evaluation of industrial oilseed biofuel feedstocks camelina, carinata, and pennycress across three fuel pathways, *Fuel*, 136, 143–155, doi:10.1016/j.fuel.2014.07.048.
- Environmental Protection Agency (2011), The 2011 National Emissions Inventory. [Available at <https://www3.epa.gov/ttnchie1/net/2011inventory.html>]
- Gordon, T. D., et al. (2014), Secondary organic aerosol production from diesel vehicle exhaust: Impact of aftertreatment, fuel chemistry and driving cycle, *Atmos. Chem. Phys.*, 14(9), 4643–4659, doi:10.5194/acp-14-4643-2014.
- Heeb, N. V., et al. (2011), Reactive nitrogen compounds (RNCs) in exhaust of advanced PM–NO_x abatement technologies for future diesel applications, *Atmos. Environ.*, 45(18), 3203–3209, doi:10.1016/j.atmosenv.2011.02.013.
- Heeb, N. V., et al. (2012), Effects of a Combined Diesel Particle Filter–DeNO_x System (DPN) on reactive nitrogen compounds emissions: A parameter study, *Environ. Sci. Technol.*, 46(24), 13,317–13,325, doi:10.1021/es3029389.
- Jaisson, S., C. Pietremont, and P. Gillery (2011), Carbamylation-derived products: Bioactive compounds and potential biomarkers in chronic renal failure and atherosclerosis, *Clin. Chem.*, 57(11), 1499–1505, doi:10.1373/clinchem.2011.163188.
- Kang, E., M. J. Root, D. W. Toohey, and W. H. Brune (2007), Introducing the concept of potential aerosol mass (PAM), *Atmos. Chem. Phys.*, 7(22), 5727–5744, doi:10.5194/acp-7-5727-2007.

- Karjalainen, P., et al. (2015), Time-resolved characterization of primary and secondary particle emissions of a modern gasoline passenger car, *Atmos. Chem. Phys. Discuss.*, 15(22), 33,253–33,282, doi:10.5194/acpd-15-33253-2015.
- Karl, M., T. Svendby, S.-E. Walker, A. S. Velken, N. Castell, and S. Solberg (2015), Modelling atmospheric oxidation of 2-aminoethanol (MEA) emitted from post-combustion capture using WRF-Chem, *Sci. Total Environ.*, 527–528, 185–202, doi:10.1016/j.scitotenv.2015.04.108.
- Karlsson, D., M. Dalene, G. Skarping, and Å. Marand (2001), Determination of isocyanic acid in air, *J. Environ. Monit.*, 3(4), 432–436, doi:10.1039/b103476f.
- Kröcher, O., M. Elsener, and M. Koebel (2005), An ammonia and isocyanic acid measuring method for soot containing exhaust gases, *Anal. Chim. Acta*, 537(1–2), 393–400, doi:10.1016/j.aca.2004.12.082.
- Lambe, A. T., et al. (2011), Characterization of aerosol photooxidation flow reactors: Heterogeneous oxidation, secondary organic aerosol formation and cloud condensation nuclei activity measurements, *Atmos. Meas. Tech.*, 4(3), 445–461, doi:10.5194/amt-4-445-2011.
- Lapuerta, M., O. Armas, and J. Rodríguez-Fernández (2008), Effect of biodiesel fuels on diesel engine emissions, *Prog. Energy Combust. Sci.*, 34(2), 198–223, doi:10.1016/j.pecs.2007.07.001.
- Li, R., et al. (2015), Modeling the radical chemistry in an oxidation flow reactor: Radical formation and recycling, sensitivities, and the OH exposure estimation equation, *J. Phys. Chem. A*, 119(19), 4418–4432, doi:10.1021/jp509534k.
- Mao, J., et al. (2008), Airborne measurement of OH reactivity during INTEX-B, *Atmos. Chem. Phys. Discuss.*, 8, 14,217–14,246.
- Mydel, P., Z. Wang, M. Brisslert, A. Hellvard, L. E. Dahlberg, S. L. Hazen, and M. Bokarewa (2010), Carbamylation-dependent activation of T cells: A novel mechanism in the pathogenesis of autoimmune arthritis, *J. Immunol.*, 184(12), 6882–6890, doi:10.4049/jimmunol.1000075.
- Ortega, A. M., D. A. Day, M. J. Cubison, W. H. Brune, D. Bon, J. A. de Gouw, and J. L. Jimenez (2013), Secondary organic aerosol formation and primary organic aerosol oxidation from biomass-burning smoke in a flow reactor during FLAME-3, *Atmos. Chem. Phys.*, 13(22), 11,551–11,571, doi:10.5194/acp-13-11551-2013.
- Peng, Z., D. A. Day, H. Stark, R. Li, J. Lee-Taylor, B. B. Palm, W. H. Brune, and J. L. Jimenez (2015), HO_x radical chemistry in oxidation flow reactors with low-pressure mercury lamps systematically examined by modeling, *Atmos. Meas. Tech.*, 8(11), 4863–4890, doi:10.5194/amt-8-4863-2015.
- Quillen, K., M. Bennett, J. Volckens, and R. H. Stanglmaier (2008), Characterization of particulate matter emissions from a four-stroke, lean-burn, natural gas engine, *J. Eng. Gas Turbines Power*, 130(5), 052807, doi:10.1115/1.2906218.
- Roberts, J. M., et al. (2010), Measurement of HONO, HNCO, and other inorganic acids by negative-ion proton-transfer chemical-ionization mass spectrometry (NI-PT-CIMS): Application to biomass burning emissions, *Atmos. Meas. Tech.*, 3(4), 981–990, doi:10.5194/amt-3-981-2010.
- Roberts, J. M., et al. (2011), Isocyanic acid in the atmosphere and its possible link to smoke-related health effects, *Proc. Natl. Acad. Sci. U.S.A.*, 108(22), 8966–8971, doi:10.1073/pnas.1103352108.
- Roberts, J. M., et al. (2014), New insights into atmospheric sources and sinks of isocyanic acid, HNCO, from recent urban and regional observations, *J. Geophys. Res. Atmos.*, 119, 1060–1072, doi:10.1002/2013JD019931.
- Robinson, A. L., N. M. Donahue, M. K. Shrivastava, E. A. Weitkamp, A. M. Sage, A. P. Grieshop, T. E. Lane, J. R. Pierce, and S. N. Pandis (2007), Rethinking organic aerosols: Semivolatile emissions and photochemical aging, *Science*, 315(5816), 1259–1262, doi:10.1126/science.1133061.
- Sarkar, C., V. Sinha, V. Kumar, M. Rupakheti, A. Panday, K. S. Mahata, D. Rupakheti, B. Kathayat, and M. G. Lawrence (2015), Overview of VOC emissions and chemistry from PTR-TOF-MS measurements during the SusKat-ABC campaign: High acetaldehyde, isoprene and isocyanic acid in wintertime air of the Kathmandu Valley, *Atmos. Chem. Phys. Discuss.*, 15(17), 25,021–25,087, doi:10.5194/acpd-15-25021-2015.
- Sennbro, C. J., C. H. Lindh, A. Östin, H. Welinder, B. A. G. Jönsson, and H. Tinnerberg (2004), A survey of airborne isocyanate exposure in 13 Swedish polyurethane industries, *Ann. Occup. Hyg.*, 48(5), 405–414, doi:10.1093/annhyg/meh034.
- Varatharajan, K., and M. Cheralathan (2012), Influence of fuel properties and composition on NO_x emissions from biodiesel powered diesel engines: A review, *Renewable Sustainable Energy Rev.*, 16(6), 3702–3710, doi:10.1016/j.rser.2012.03.056.
- Verbrugge, F. H., W. H. W. Tang, and S. L. Hazen (2015), Protein carbamylation and cardiovascular disease, *Kidney Int.*, 88(3), 474–478, doi:10.1038/ki.2015.166.
- Veres, P., J. M. Roberts, C. Warneke, D. Welsh-Bon, M. Zahniser, S. Herndon, R. Fall, and J. de Gouw (2008), Development of negative-ion proton-transfer chemical-ionization mass spectrometry (NI-PT-CIMS) for the measurement of gas-phase organic acids in the atmosphere, *Int. J. Mass Spectrom.*, 274(1–3), 48–55, doi:10.1016/j.ijms.2008.04.032.
- Veres, P., J. M. Roberts, I. R. Burling, C. Warneke, J. de Gouw, and R. J. Yokelson (2010), Measurements of gas-phase inorganic and organic acids from biomass fires by negative-ion proton-transfer chemical-ionization mass spectrometry, *J. Geophys. Res.*, 115, D23302, doi:10.1029/2010JD014033.
- Veres, P. R., and J. M. Roberts (2015), Development of a photochemical source for the production and calibration of acyl peroxyoxynitrate compounds, *Atmos. Meas. Tech.*, 8(5), 2225–2231, doi:10.5194/amt-8-2225-2015.
- Wang, Z., S. J. Nicholls, E. R. Rodriguez, O. Kumm, S. Hörkkö, J. Barnard, W. F. Reynolds, E. J. Topol, J. A. DiDonato, and S. L. Hazen (2007), Protein carbamylation links inflammation, smoking, uremia and atherogenesis, *Nat. Med.*, 13(10), 1176–1184, doi:10.1038/nm1637.
- Wentzell, J. J. B., J. Liggio, S.-M. Li, A. Vlasenko, R. Staebler, G. Lu, M.-J. Poitras, T. Chan, and J. R. Brook (2013), Measurements of gas phase acids in diesel exhaust: A relevant source of HNCO?, *Environ. Sci. Technol.*, 47(14), 7663–7671, doi:10.1021/es401127j.
- Westberg, H., H. Löfstedt, A. Seldén, B.-G. Lilja, and P. Nayström (2005), Exposure to low molecular weight isocyanates and formaldehyde in foundries using hot box core binders, *Ann. Occup. Hyg.*, 49(8), 719–725, doi:10.1093/annhyg/mei040.
- Woodward-Massey, R., Y. M. Taha, S. G. Moussa, and H. D. Osthoff (2014), Comparison of negative-ion proton-transfer with iodide ion chemical ionization mass spectrometry for quantification of isocyanic acid in ambient air, *Atmos. Environ.*, 98, 693–703, doi:10.1016/j.atmosenv.2014.09.014.
- Young, P. J., L. K. Emmons, J. M. Roberts, J.-F. Lamarque, C. Wiedinmyer, P. Veres, and T. C. VandenBoer (2012), Isocyanic acid in a global chemistry transport model: Tropospheric distribution, budget, and identification of regions with potential health impacts, *J. Geophys. Res.*, 117, D10308, doi:10.1029/2011JD017393.
- Zhao, R., et al. (2014), Cloud partitioning of isocyanic acid (HNCO) and evidence of secondary source of HNCO in ambient air, *Geophys. Res. Lett.*, 41, 6962–6969, doi:10.1002/2014GL061112.